CFD SIMULATION OF A DRY SCROLL VACUUM PUMP INCLUDING LEAKAGE FLOWS

Jan HESSE*, Rainer ANDRES

CFX Berlin Software GmbH,
Berlin, Germany
jan.hesse@cfx-berlin.de

* Corresponding Author

ABSTRACT

One challenge for the numerical simulation of a dry scroll vacuum pump is the discretization of the chamber volume, which changes with time. In addition, the flow characteristics are very complex including the leakage flow caused by radial and axial gaps between the rotors and the housing. For engineers and designers it is imperative to understand the influence of such leakage flows on the efficiency of the dry scroll vacuum pump.

This paper describes the workflow for Computational Fluid Dynamics (CFD) of a dry scroll vacuum pump and shows some preliminary results. The computational grids for the time dependent flow volume are generated by the grid generator TwinMesh. The meshing software generates and optimises all necessary grids for each time step prior to the actual simulation and calculates the mesh quality to assure high quality numerical results. Furthermore, the grid generation accurately considers axial gaps.

The transient numerical simulations are performed by the commercial CFD software code ANSYS CFX, which is able to handle complex flow characteristics. The simulations consider compressibility, turbulence, and heat transfer effects using ideal gas properties for the fluid. The pressure ratio between inlet and outlet is varied as well as the gap size. The results are compared with analytical methods. This paper shows time dependent information such as pressure, velocity, and temperature for specific locations in the chamber volume and also integral values such as power, torque, and mass flow. Finally, cross-sectional views are presented for different positions and time steps.

1. INTRODUCTION

Nowadays, dry scroll vacuum pumps (DSPV) are essential devices in many different industrial and academic processes. The electronic and semiconductor industry is the biggest application area of vacuum pumps, for example plasma etching and physical vapour deposition in manufacturing displays or computer chips. Vacuum pumps are also used in food industry for packaging technology or freeze-drying, in metallurgy for degassing of melt or inside a coating line. For research vacuum technology is used for electron microscopes or mass spectrometer. There are several different types of compressor mechanism. The scroll pump is constructively the simplest solution for a vacuum pump. The advantages are high performance down to 10^{-3} mbar, low cost, easy maintenance, low noise and small vibrations compared with other kinds of dry vacuum pumps.

The scroll vacuum pump is quit complex from the fluid dynamics point of view. The driven orbiting scroll wrap changes the position relative to the fixed scroll wrap which results in a time changing working chamber volume. The fluid is compressible and therefore acoustic aspects could be important. Because of the vacuum characteristics the transition from the continuous flow regime to the molecular regime has to be taken into account. Though Computational Fluid Dynamics (CFD) is a broadly accepted tool, both in academia as well as in industry, to analyze fluid mechanics in complex systems in order to visualize the flow, understand and optimize such systems, it is so far rarely used in industry for the examination and improvement of scroll machines.

The numerical computation of screw machines requires accurate grid generation because the fluid flow is transient and depends on the rotor position. Furthermore, the grid needs a high resolution especially in the gaps and their vicinity. Consequently, TwinMesh was developed with the aim to generate high quality grids in a short time. As a result, CFD can now be utilized on a day-to-day basis in industrial applications of PD machines.

This paper is based on the paper of Yue et al. (2015) which includes CFD simulation results of a dry scroll vacuum pump. In addition the axial gaps are included in the simulation domain.

2. GEOMETRY

The working chamber of the scroll pump is a simple cylindrical volume including one fixed and one orbiting scroll wrap. The inlet and outlet volume is simplified as a pipe, which could have an influence on the DSPV performance in comparison to the real geometry. One important geometrical parameter of DSVP is the volume ratio, which is the ratio of the suction chamber volume to the discharge chamber volume. Here a volume ratio of 2.0 is used corresponding to the involute starting angle Φ_S of 3π like in Yue et al. (2015) and Li et al. (2010, Vacuum 84). The pressure inside the working chamber is analyzed on four different locations (orbiting angle of 300°, 570°, 840° and 1110°) next to the fixed scroll wrap, which are the pressure transducer locations of Li et al. (2010, Vacuum 84). The used axial clearance size is 30 micron. The specified axial clearance in the paper of Li et al. (2010, Vacuum 84) of 300 micron must be a mistake.

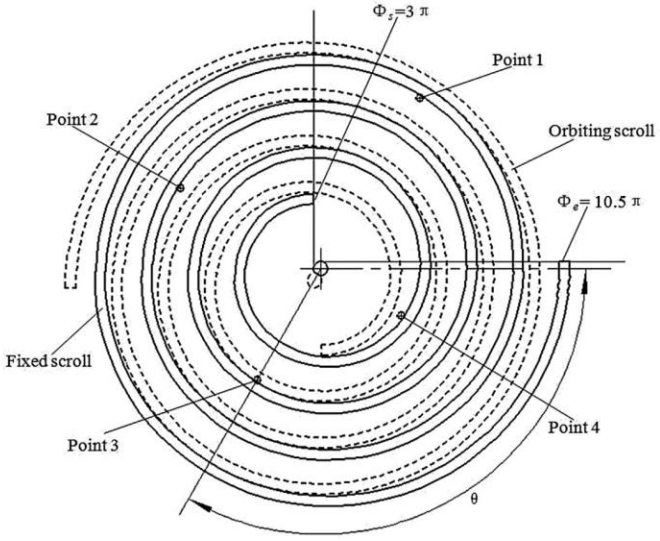

Figure 1: Geometry of the scroll wraps (Yue et al., 2015)

Table 1: Basic parameters of the DSVP

Items	Value
Radius of the basic circle	3 mm
Pitch of involute	18.85 mm
Initial angle of involute	40°
Thickness of scroll wrap	4.19 mm
Height of the scroll wrap	30 mm
Loops of scroll	5.25
Axial clearance	0.03 mm
Minimum radial clearance	0.036 mm

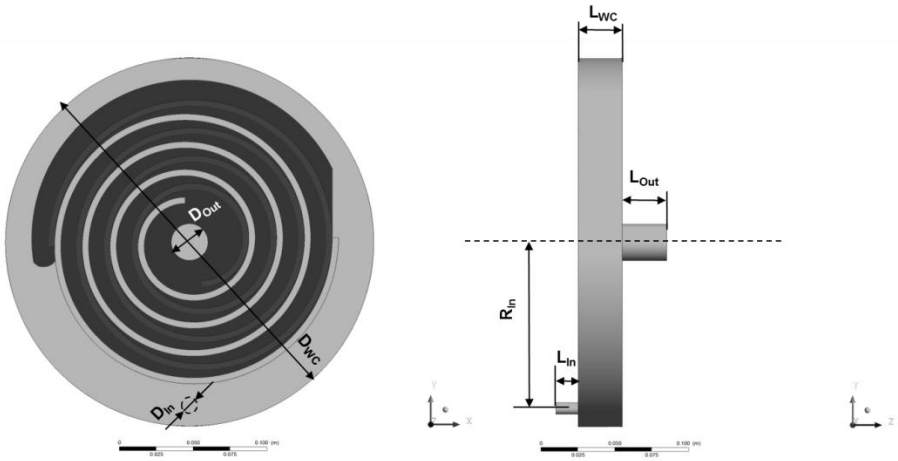

Figure 2: Geometry of the simulation domain

Table 2: Parameters of the simulation domain

Items	Value [mm]
L_{In}	15
L_{WC}	30
L_{Out}	30
R_{In}	112.5
D_{In}	8
D_{WC}	250
D_{Out}	25

3. MESHING

The discretization of the fluid volume is the main challenge to get reliable simulation results. The time changing volume has to be represented by a numerical mesh including all gaps. There are several methods to model the chamber volume with different restrictions.

3.1 Chamber Modeling

The immersed solid method is a comfortable method to setup a simulation including rotor movement. This method needs only a background mesh (without solid of orbiting scroll) and a mesh for scroll wrap solid body. A momentum source forces the fluid to the rotor movement in regions where the solid mesh overlaps with the background mesh. There are a lot of restrictions for the immersed solid method. For example it can only be used for single-phase incompressible fluids. The background mesh needs a fine mesh near the wall to represent the gap region. This method cannot model the compressibility effects of a DSPV.

The remeshing method generates a mesh during the simulation depending on the mesh quality of the deformed mesh for each time step. In comparison to the immersed solid method compressible simulations are allowed also including multi-phase. The main disadvantage is that remeshing is necessary for almost each time step when having small gaps. The time step has to be small to reach an acceptable deformed mesh per time step. This method is not efficient for a CFD simulation of a DSPV.

The method to use pre-generated meshes for each rotor position is the best method for the simulation of a DSPV. This can be done by hand (ANSYS ICEM CFD Hexa) or with special meshing programs like TwinMesh which has a more automatic approach. Structured meshes are generated before doing the simulation and imported later at the beginning of each time step of the simulation. The computational effort is minimized und the mesh quality is high leading to reliable simulation results.

3.2. Simulation Domain

The simulation domain is split into different volumes to use the adequate meshing strategy for each volume (Figure 3). The mesh of the stator domain is generated with ANSYS Meshing including the inlet and outlet pipes and the stationary part of the working chamber and the axial gap of the fixed scroll. The mesh of the rotor domain is created with TwinMesh whereas the axial gap of the rotor is generated with ANSYS Meshing as well.

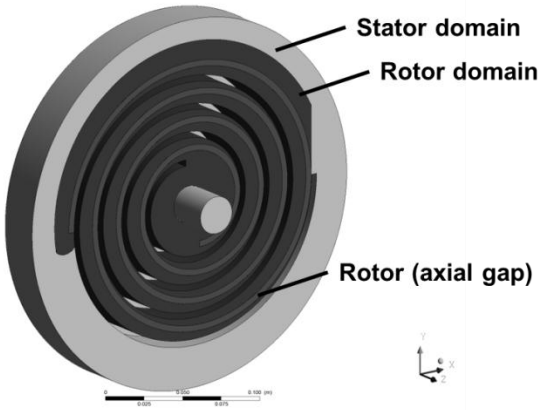

Figure 3: Simulation domains

TwinMesh is a meshing software for PD machines with two axially parallel rotors, with complex rotor geometry, i.e. continuous (e.g. lobe pump), discontinuous (e.g. screw compressor) or with a single rotor (e.g. scroll compressor, eccentric screw pump). CAD data of the rotor and casing curvature can be imported and is used for the structured grid generation. The topology of a scroll is meshed using O-type grid around the rotor curvature. Figure 4 shows the TwinMesh GUI in the case of a scroll pump. TwinMesh generates 2D meshes for each rotation angle of the rotor with the same topology and node numbers including a refined boundary layer resolution layers towards rotor and housing walls. The meshes are smoothed with an explicit and iterative method to reach homogeneous node distribution and orthogonality. The resulting mesh of the chamber volume can be analyzed by quality criteria, such as minimum element angle, aspect ratio and volume change of cells. The 2D meshes are used to get the 3D volume mesh. The 3D meshes are exported from TwinMesh for each rotor position (i.e. the meshes cover one complete rotation), where an angle increment of 1° is used for the simulation of the dry scroll vacuum pump.

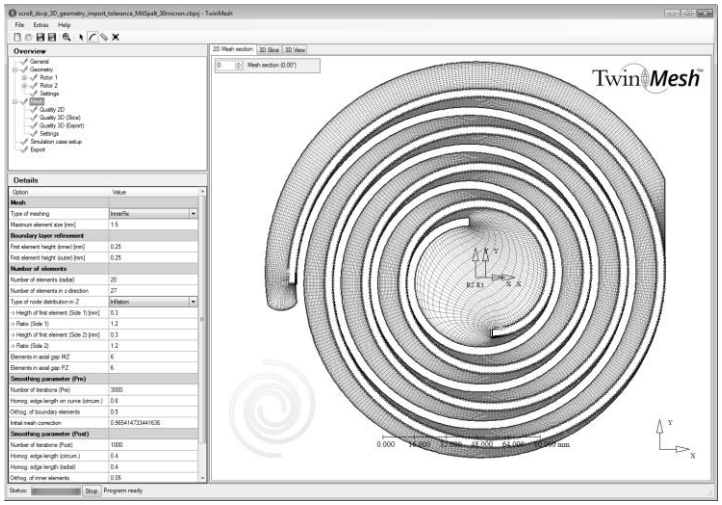

Figure 4: TwinMesh GUI (2D cross section)

4. SIMULATION SETUP

The commercial CFD solver ANSYS CFX is used for the simulation. The meshes for the stator and rotor domain are imported in the setup and connected with a GGI (Generalized Grid Interface) to consider the time step dependent connection, where the flux of mass, momentum, heat and turbulence are conserved. For the definition of the boundary condition the pressure and the temperature at inlet and outlet are specified as well as the rotational speed of the rotating scroll wrap. The wall boundary condition is set to no slip wall, which is correct for viscous flow (Kn<0.01). The wall temperature is set to 65°C for almost all simulations. Three different values for the suction pressure are used (17 kPa, 42 kPa, 95 kPa) and a discharge pressure of 95 kPa to compare the results with the measurement from Li et al. (2010,Vacuum 85). The lowest suction pressure is 17 kPa which results to Kn=0.011. The inlet temperature is 20°C for each simulation. The rotational speed is 1704 rpm. The fluid is defined as ideal gas with constant properties beside the density. The SST turbulence model is used to take turbulence in the free flow into account, whereas the turbulent kinetic energy goes to zero inside the clearances. The advection scheme is high resolution and the transient scheme is second order backward euler.

The mesh deformation due to the orbiting scroll movement is realized by a FORTRAN routine, which imports the point coordinate data (TwinMesh export files) for each node and each time step of the rotor domain. Therefore no interpolation is needed between the time steps leading to a simulation result without interpolation errors.

5. SIMULATION RESULTS

The simulation results are compared with the results of Li et al. (2010, Vacuum 84 and 85) and Yue et al. (2015). First the working process of the DSPV is analyzed. Figure 5 shows the CFD simulation results of Yue et al. (2015) in comparison to the measurements of Li et al. (2010, Vacuum 85) for a rotational speed of 1704 rpm. They use a different discharge pressure for measurement (95 kPa) and CFD simulation (101 kPa) leading a pressure offset for point 4. In the measurement the increase of the pressure with the rotation angle θ is larger than the increase of the CFD pressure curve. In CFD the pressure decrease from the high pressure chamber to the lower pressure chamber (scroll wrap passes the measurement location) is faster than the measured pressure curve. The curves of point 2 and point 3 have a pressure jump at every 360°, which indicates non periodic simulation results of the pressure curve (range of 360° results linked together). It is not clear why the pressure decrease for each measurement point starts before the rotor is passing the pressure transducer position (Rotation angle position of 30° P4, 120° P3, 210° P2, 300° P1). The paper of Li et al. (2010, Vacuum 85) has no information about the triggering of the rotation angle with the measurements. It could be that the pressure transducer information has a wrong link to the rotation angle, which results in an offset along the x-axis or there are other geometrical details (deformation of the scroll) which are important but unknown.

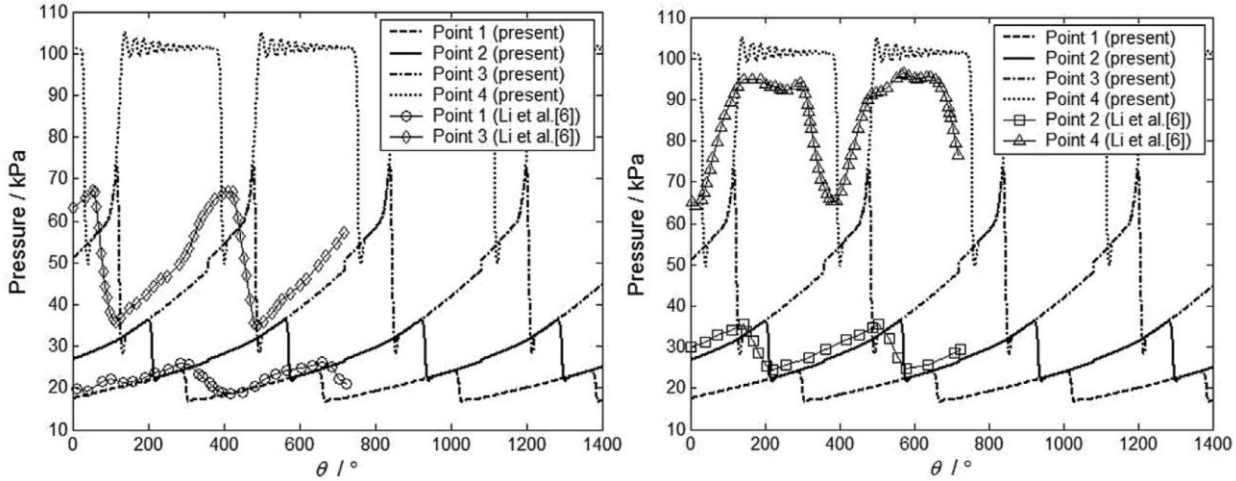

Figure 5: Working process (suction pressure 17kPa, 1704 rpm) (Yue et al., 2015)

5.1 Working Process

The working process of a DSVP describes the pressure increase with the change of the rotation position of the orbiting scroll wrap. The geometry of the DSPV used in this paper is designed for a pressure ratio of 2.64 (Yue et al., 2015) between the inlet and outlet pressure. A higher pressure ratio leads to under-compression (inlet pressure of 17 kPa) whereas a lower pressure ratio leads to over-compression. Figure 6 shows the pressure change at the measurement positions depending on the rotation angle. Our CFD results are compared with the CFD results of Yue at al. (2015). The simulation conditions are nearly the same as good as available in the referenced paper (Yue et al., 2015) except the outlet pressure. The pressure increase of our simulation is a bit slower than described in the paper. The reason could be the non-periodic working cycle of the paper results (more time step needed), differences in the boundary conditions or the different pressure ratio.

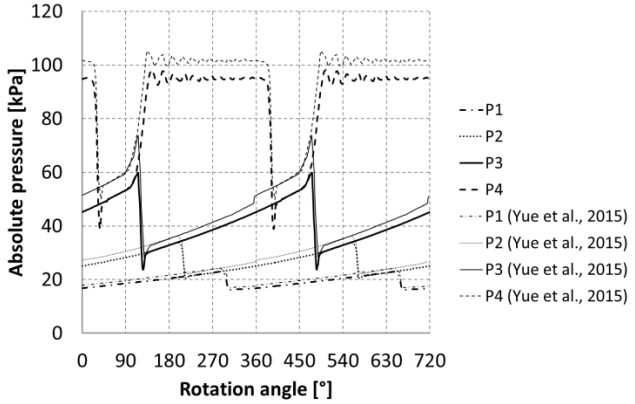

Figure 6: Comparison of our simulation results with the CFD results of Yue et al. (2015)
(no axial gaps, RNG turbulence model, suction pressure is 17 kPa, rotational speed is 1704 rpm)

Based on that setup the axial gaps are included. First we start with the specified unusual axial gap size (300 micron) described in the papers to clarify the possible mistake. Figure 7 shows the working process. The axial gap is too large to handle the pressure ratio. For further investigation we use 30 micron for the axial gap size and switch to the SST turbulence model.

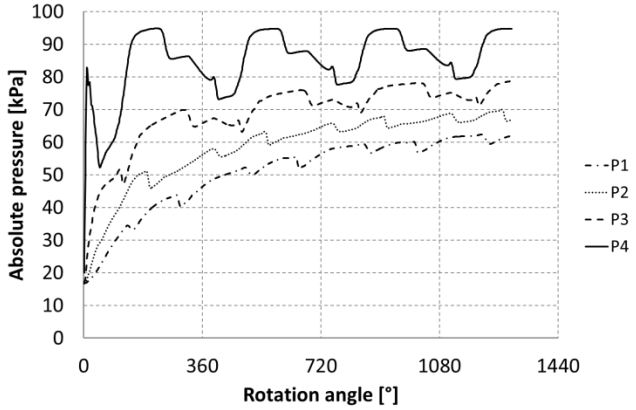

Figure 7: Pressure increase using axial gap size of 300 micron
(suction pressure is 17 kPa, rotational speed is 1704 rpm)

The comparison of our CFD results (considering the axial gaps) with the measurement results including a correction shift along the x-axis shows a good agreement (Figure 8). The correction shift is necessary to have the same pressure drop position where the orbiting scroll wrap passes the pressure transducer positon. The pressure drop in the measurements location of Li et al. (2010, Vacuum 85) and the pitch between the locations were not appropriate to the geometric definition of the transducer position.

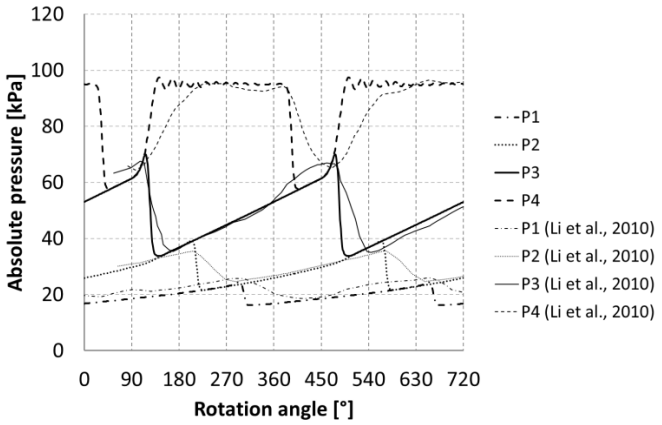

Figure 8: Comparison of our CFD results with measurements of Li et al. (2010, Vacuum 85)

The gradient of the pressure decrease in the measurement data is smaller than in CFD. This is due to the fact that the pressure transducer is connected via a pressure hole in the fixed scroll with a specific diameter and is located in a specific distance to the fixed scroll wrap (Li et al., 2010, Vacuum 85). If the orbiting scroll wrap passes the pressure hole the pressure transducer measures the area averaged pressure in the axial clearance. This leads to a slower pressure decrease. A comparable post processing of the CFD results using the averaged pressure on a circle plane located at a distance half of the scroll wrap thickness gives a comparable working process.

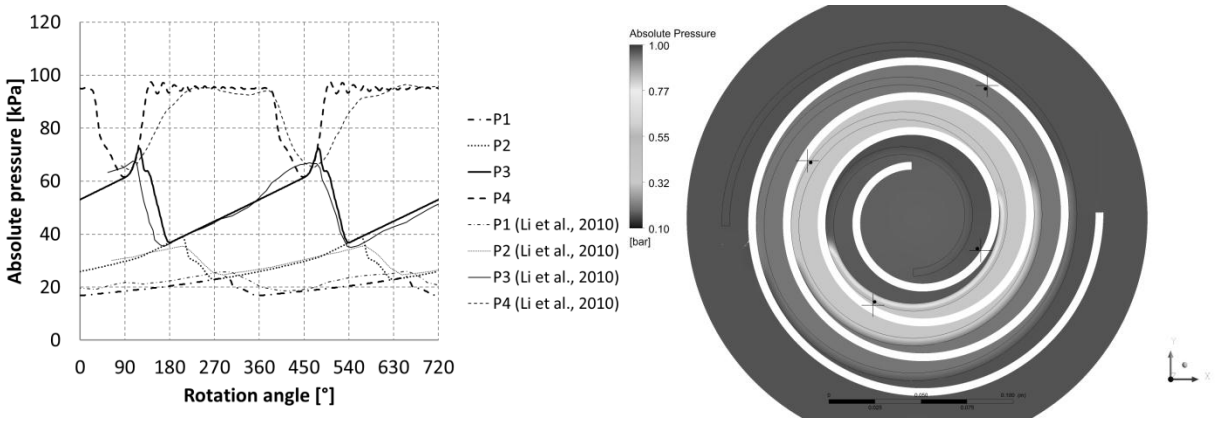

Figure 9: Average pressure calculation (left), slice plane in the axial gap (right) on fixed scroll side with measurement locations (dots) and CFD monitor point (crosses)

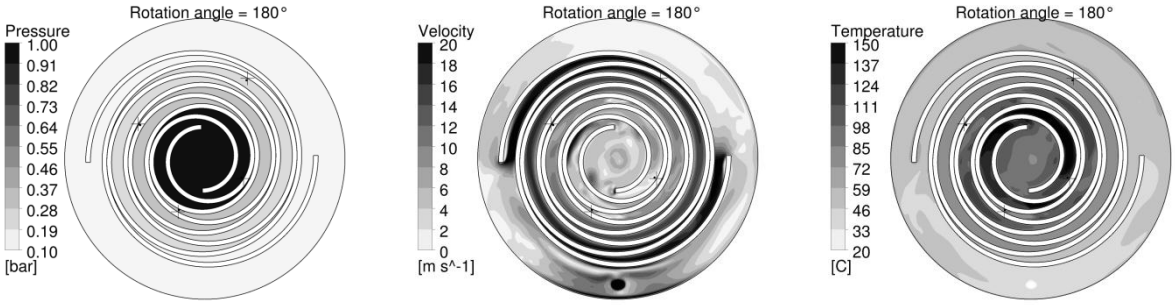

Figure 10: Cross-sectional view of the pressure (left), velocity (middle) and temperature (right) (rotation angle of 180°, suction pressure of 17 kPa and rotational speed of 1704 rpm)

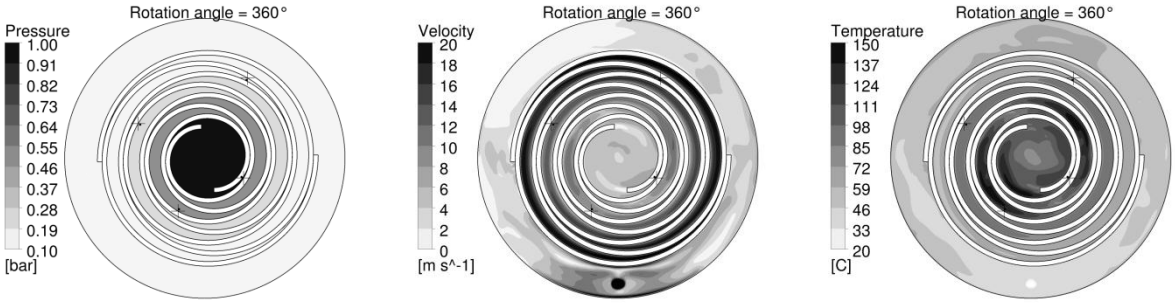

Figure 11: Cross-sectional view of the pressure (left), velocity (middle) and temperature (right) (rotation angle of 360°, suction pressure of 17 kPa and rotational speed of 1704 rpm)

Figure 10 and 11 show the pressure, temperature and velocity for two different rotor positions.

The comparison of our CFD results with the theoretical approach of Li et al. (2010, Vacuum 85) shows a difference in the working process. The pressure increase is faster than in the CFD results. The specification of the temperature behavior has a main influence on the pressure increase.

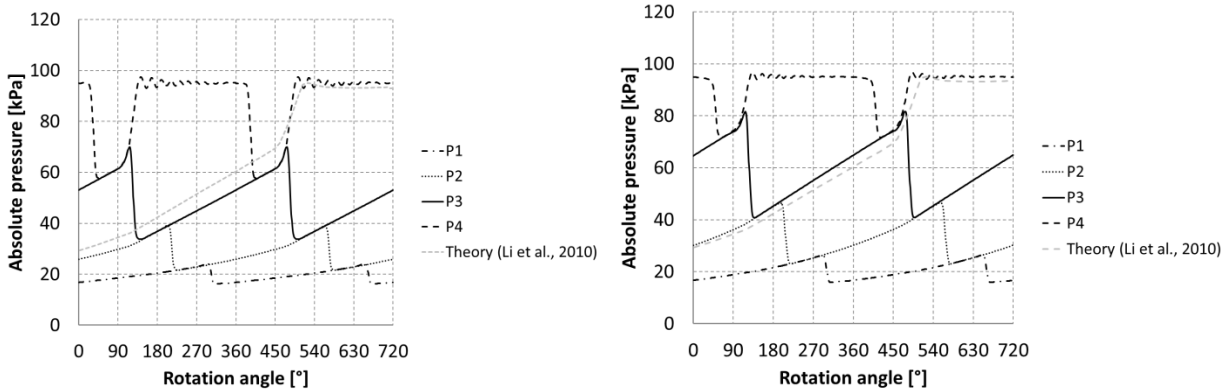

Figure 12: Comparison of theoretical approach of Li et al. (2010, Vacuum 85) with our CFD results using a wall temperature of 65°C (left) and an adiabatic wall (right)

With an adiabatic simulation the pressure increase is faster in comparison to the theoretical process due to the higher temperatures (no cooling over the casing). The correct modelling of the heat transfer from the internal fluid to the ambient is really important to get the correct working process.

5.2 Mass Flow

The mass flow decreases with decreasing suction pressure.

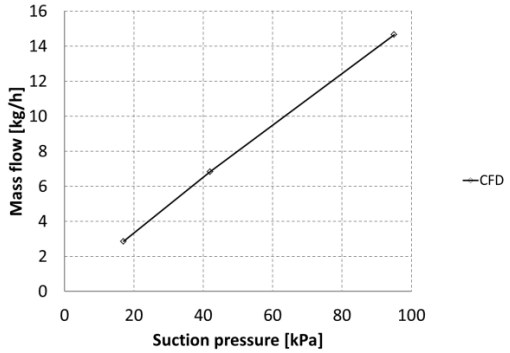

Figure 13: Mass flow from CFD results (rotational speed of 1704 rpm)

5.3 Torque

Figure 14 shows the instantaneous torque of orbiting scroll under different suction pressures.

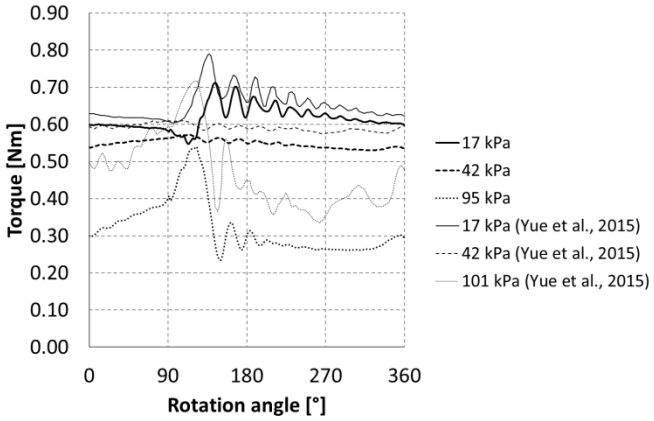

Figure 14: Torque on orbiting rotor from our CFD results in comparison to the CFD results of Yue et al. (2015) (rotational speed of 1704 rpm)

Table 3: Power consumption

Suction pressure kPa	Power consumption W	Reference
17	110.3	CFD results
42	96.4	CFD results
95	54.6	CFD results
31	174	Polytropic process
17	116.6	CFD Yue et al. (2015)
42	105.6	CFD Yue et al. (2015)
101	84.1	CFD Yue et al. (2015)

6. CONCLUSIONS AND OUTLOOK

This paper shows CFD results for a dry scroll vacuum pump including axial gaps. Different suction pressures from 17 kPa to 95 kPa were applied using an inlet temperature of 20°C. The CFD results of the working process are compared with theoretical calculation and experimental data. In addition, average values of the mass flow and power consumption are shown for different suction pressures. For the CFD simulation ANSYS CFX was used and the meshes for the working chamber were created with the meshing software TwinMesh and the stator meshes with ANSYS Meshing.

The comparison of the CFD results with the experimental data indicates that the working mechanism and flow conditions within the dry scroll vacuum pump are well captured by the simulation. The heat transfer from the process gas to the ambient over the casing has a main impact on the increase of the pressure over the rotation angle. The pressure increase of the adiabatic process is faster than specifying a constant wall temperature.

Further investigation will focus on the heat transfer through the casing of the pump, to have the correct solid and fluid temperature depending on the rotational speed. If the boundary conditions including the heat transfer are specified more accurate further investigations are planned for a mesh refinement study also including real gas properties.

NOMENCLATURE

Kn	knudsen number	()
θ	rotation angle	(°)

REFERENCES

Li, Zeyu & Li, Liansheng & Zhao, Yuanyang & Bu, Gaoxuan & Shu, Pengcheng, 2010, Theoretical and experimental study of dry scroll vacuum pump, *Proceedings of the Vacuum 84*, (415-421), Elsevier

Li, Zeyu & Li, Liansheng & Zhao, Yuanyang & Bu, Gaoxuan & Shu, Pengcheng & Lui, Jinping, 2010, Test and analyses on the working process of dry scroll vacuum pump, *Proceedings of the Vacuum 85*, (95-100), Elsevier

Yue, Xiang-Ji & Lu, Yan-jun & Zhang, Ying-Li & Ba, De-chung & Wang, Guang-Yu, 2015, Computational fluid dynamics simulation study of gas flow in dry scroll vacuum pump, *Proceedings of the Vacuum 116*, (144-152), Elsevier